Matthew, J. B. (1978) Ph.D. Thesis, Indiana University, Bloomington, IN.
Matthew, J. B., Morrow, J. S., Wittebort, R. J., & Gurd, F. R. N. (1977) *J. Biol. Chem. 252*, 2234.
Matthew, J. B., Hanania, G. I. H., & Gurd, F. R. N. (1978a) *Biochem. Biophys. Res. Commun. 81*, 410.
Matthew, J. B., Friend, S. H., Botelho, L. H., Lehman, L. D., Hanania, G. I. H., & Gurd, F. R. N. (1978b) *Biochem. Biophys. Res. Commun. 81*, 416.
Matthew, J. B., Hanania, G. I. H., & Gurd, F. R. N. (1979) *Biochemistry* (following paper in this issue).
Morrow, J. S., Matthew, J. B., Wittebort, R. J., & Gurd, F. R. N. (1976) *J. Biol. Chem. 251*, 477.
Muirhead, H., Cox, J. M., Mazzarella, L., & Perutz, M. F. (1967) *J. Mol. Biol. 28*, 117.
O'Donnell, S., Mandaro, R., & Schuster, T. (1978) *Biophys. J. 21*, 201a.
Orttung, W. H. (1968) *J. Phys. Chem. 72*, 4066.
Orttung, W. H. (1969) *J. Am. Chem. Soc. 91*, 162.
Orttung, W. H. (1970) *Biochemistry 9*, 2394.
Perutz, M. F. (1970) *Nature (London) 228*, 726.
Perutz, M. F. (1977) *BioSystems 8*, 261.
Riggs, A., & Atha, D. H. (1976) *J. Biol. Chem. 251*, 5537.
Rollema, H. S., de Bruin, S. H., Janssen, L. H. M., & van Os, G. A. J. (1975) *J. Biol. Chem. 250*, 1333.
Rosemeyer, M. A., & Huehns, E. R. (1967) *J. Mol. Biol. 25*, 253.
Schneider, R. G., Alperin, J. B., Brimhall, B., & Jones, R. T. (1969) *J. Lab. Clin. Med. 73*, 616.
Shire, S. J., Hanania, G. I. H., & Gurd, F. R. N. (1974a) *Biochemistry 13*, 2967.
Shire, S. J., Hanania, G. I. H., & Gurd, F. R. N. (1974b) *Biochemistry 13*, 2974.
Shire, S. J., Hanania, G. I. H., & Gurd, F. R. N. (1975) *Biochemistry 14*, 1352.
Tanford, C. (1957) *J. Am. Chem. Soc. 79*, 5340.
Tanford, C. (1961) *Physical Chemistry* of *Macromolecules*, Chapter 8, Wiley, New York.
Tanford, C., & Kirkwood, J. G. (1957) *J. Am. Chem. Soc. 79*, 5333.
Tanford, C., & Nozaki, Y. (1966) *J. Biol. Chem. 241*, 2832.
Tanford, C., & Roxby, R. (1972) *Biochemistry 11*, 2192.
Wittebort, R. J., Rothgeb, T. M., Szabo, A., & Gurd, F. R. N. (1979) *Proc. Natl. Acad. Sci. U.S.A. 76*, 1059.

Electrostatic Effects in Hemoglobin: Bohr Effect and Ionic Strength Dependence of Individual Groups†

James B. Matthew,‡ George I. H. Hanania,§ and Frank R. N. Gurd*

ABSTRACT: The electrostatic treatment applied in the preceding paper in this issue [Matthew, J. B., Hanania, G. I. H., & Gurd, F. R. N. (1979) *Biochemistry* (preceding paper in this issue)] to the titration behavior of individual groups in human deoxyhemoglobin and oxyhemoglobin was applied to the computation of the alkaline Bohr effect at various values of ionic strength. The enhanced proton binding of deoxyhemoglobin in the pH range of 6–9 was accounted for at ionic strength 0.01 M by the effects of the unique charge distributions of ionizable groups in the two quaternary states. At ionic strength 0.10 M the effects of 2–4 bound anions had to be considered in addition in the deoxyhemoglobin charge configuration. At the higher ionic strength 10 groups per tetramer contributed to the Bohr effect, whereas 28 groups were contributory at the lower ionic strength. The ionic strength dependence of individual groups in the two tetrameric structures as well as in the α-chain monomer was explained in terms of the electrostatic treatment. This examination showed that the differences in electrostatic behavior of deoxy- and oxyhemoglobin follow from particular dissymmetries in their configurations with respect to charge and static solvent accessibility.

The preceding paper in this issue (Matthew et al., 1979) introduced the application to human hemoglobin of a modified discrete-charge electrostatic model. The characteristics of the protein–solvent interface are taken into account by an approximation incorporating the static solvent accessibility of each charged site as computed from the crystallographic structure of the protein. A basic feature of the model is that the charge and the pK_i of each ionizable group vary with pH and ionic strength. Hence, the charge-related properties of the protein incorporate, to some degree, individual contributions from all these groups. Examples of the computed contribution of each ionizable group in the hemoglobin molecule to the pK_i of a given group were presented for several different pH values. The computed pK_i values under certain conditions of interest were tabulated for all ionizable groups in the deoxy- and oxyhemoglobin tetramers, and correspondence with observed values was established in those cases where comparison was possible. The titration curves computed as functions of ionic strength for the deoxyhemoglobin and oxyhemoglobin tetrameric structures agreed with experimental values.

The present paper explores in greater detail the application of the model to elucidating differences in the electrostatic behavior of the deoxyhemoglobin and oxyhemoglobin structures. To account for the alkaline Bohr effect, that describes the excess of proton binding by deoxyhemoglobin relative to oxyhemoglobin in the physiological pH range (Bohr et al., 1904), it is necessary to invoke the intervention of at most two bound chloride ions (per $\alpha\beta$ dimer) in addition to the direct

† From the Department of Chemistry, Indiana University, Bloomington, Indiana, 47405. *Received November 9, 1978; revised manuscript received February 16, 1979.* This is the 105th paper in a series dealing with coordination complexes and catalytic properties of proteins and related substances. For the preceding paper see Matthew et al. (1979). This work was supported U.S. Public Public Health Service Research Grant HL-05556. J.B.M. was supported by U.S. Public Health Service Grant T01 GM-1046.

‡ Present address: Department of Molecular Biophysics and Biochemistry, Yale University, New Haven, CT.
§ Present address: Department of Chemistry, American University of Beirut, Beirut, Lebanon.

0006-2960/79/0418-1928$01.00/0

effects of the quaternary transition on the charged-site geometries. The contributions of five individual ionizable groups per $\alpha\beta$ dimer are shown to be of primary importance. Close examination of the effects of variations in ionic strength brings out the most novel observation from this theoretical study. This is that the general nature of the differences between the electrostatic behavior of the deoxyhemoglobin and oxyhemoglobin tetrameric forms follows from a particular configuration of ionizable groups that is somewhat more exaggerated in the deoxyhemoglobin quaternary structure than in the oxyhemoglobin quaternary structure. These properties have been explored with simulated models and by comparison of the electrostatic characteristics of the monomeric deoxyhemoglobin α chain with those of the much more symmetrical configuration in myoglobin.

Electrostatic Computations

Free energies of interaction of the ionizable groups in several proteins have been calculated (Matthew, 1978; Matthew et al., 1978a,b), according to the procedures described in the preceding paper in this issue (Matthew et al., 1979), from atomic coordinates obtained from the Brookhaven Protein Data Bank. With the exception of the terminal α-amino groups in hemoglobin tetramers for which pK_{int} was taken as 7.00 (Gros & Bauer, 1978), the same set of pK_{int} values was used throughout. Theoretical hydrogen ion titration curves for individual sites were generated as already described (Matthew et al., 1979). The treatment adjusts the characteristic pK_{int} for the ionizable group in question to the effective pK_i at a given pH by the inclusion of an electrostatic ΔpK_i term reflecting the sum of electrostatic free energy contributions, W'_{ij}, between the particular group i and all other groups j. W'_{ij} is the same as that computed from the Tanford–Kirkwood treatment (Tanford & Roxby, 1972), W_{ij}, multiplied by the factor 1 − SA where SA is the fractional static solvent accessibility. Computed pK_i values are sometimes expressed as $pK_{1/2}$, those values applying at the pH of half-titration. The charge borne on a given site, Z_i or Z_j, varies between −1 and 0 or 0 and +1 to allow for fractional saturation. Net sums of charges are expressed as $\bar{Z}$, for example, in titration curve plots.

Bound Chloride Ions. The presence of bound anions such as chloride requires special consideration since the anions contribute to Coulombic influences without representing in themselves sites for proton binding. Ambiguity could arise because of uncertainty about the thermodynamics of anion binding and about the pH dependence of the binding equilibrium, particularly so if the binding site involves more than a single, anchoring positive group.

Chloride ion at the 0.10 M level is known to saturate a site Val-1α_1···Cl^-···Arg-141α_2 in deoxyhemoglobin tetramer (Arnone et al., 1976; O'Donnell et al., 1978) in which it is presumably bound by the two positively charged groups but would not be bound by the form in which both groups were in the neutral base form. In the presence of the chloride ion, the calculated $pK_{1/2}$ for Val-1α is 8.00 and for Arg-141α it is over 12.0. At pH values near 9 where Val-1α will be substantially deprotonated in any event but not Arg-141α, computations were made with the chloride ion included or excluded from the site in question. The effect was found to be small, amounting to only 0.05 proton equiv at pH 9.0. Another chloride binding site in deoxyhemoglobin at His-117β (Hayashi et al., 1974; Tucker & Perutz, 1977) was taken into account. However, the combined effect of the four chloride ions per tetramer when both Val-1α and His-117β were deprotonated amounted to no more than 0.06 proton equiv in the range of pH 7–9. Accordingly, for purposes of calculation, the chloride sites were taken to be occupied by the anion over the pH range up to near pH 10 where their inclusion would begin to repress the deprotonation of one or more lysine residues.

A number of other positively charged sites have been implicated in chloride binding under various conditions of pH, ionic strength, and salt concentration. Perhaps the most noteworthy is a possible low-affinity site in the β-cleft region in the oxyhemoglobin tetramer (Chiancone et al., 1976; Wiechelman et al., 1978). This site, probably involving residues His-143β, Lys-82β, and Val-1β, could contribute under some conditions to the acid Bohr effect (Rollema et al., 1975).

Simulated Titration Curves. One of the striking observations in the present work is that the effect of ionic strength on hydrogen ion titration curves of hemoglobin varies significantly from classical expectations. Protein titration curves are known to be subject to salt effects usually in such a way that the pH region near the isoelectric point shows minimum dependence on ionic strength. This behavior is predicted by application of Debye–Hückel theory to the smeared charge model of globular proteins (Tanford, 1965). As Figure 4 of the preceding paper in this issue shows (Matthew et al., 1979), this is not the case for hemoglobin, although myoglobin and cytochrome *c* do indeed follow the classical pattern (Shire et al., 1974a,b; Matthew, 1978). To test whether deviation from classical ionic strength effects is related to nonuniform distribution of charged sites on the protein, simulated titration curves for certain model systems were computed.

Various charge distributions were simulated, by using the same model and formalism that were applied to the protein (Matthew et al., 1979). In a typical computation, a uniform (symmetric) charge distribution was achieved by placing 14 point charges on the vertexes of a 24-faced regular polyhedron inscribed within a low dielectric sphere of radius 10.0 Å. The sites were assigned pK_{int} values to simulate amino acid residues: 4.00 for acidic groups, 10.40 or 12.00 for basic groups, and 6.00 or 6.60 for intermediate histidine-like groups. A mean static accessibility fraction, SA, of 0.50 was used for many of the trials; varying this value for all point charges together does not alter the overall form of the results, but separate variation for specific sites produces profound effects as described below. Nonuniform charge distributions were simulated by pairing oppositely charged groups at an ion-pair distance of 3.0 Å. Interactions were also modulated by reducing the solvent accessibilities of ion-paired groups to 0.20. Dielectric constants used for the protein were $D_i = 4.0$ and $D = 78.5$ at 25 °C. Since the sphere had a radius of 10.0 Å, the ion exclusion radius was taken to be 12.0 Å. Calculations of electrostatic free energies, effective pK_i values, and charges z_i, as functions of pH and ionic strength, were then made according to the procedure already described (Matthew, 1978; Matthew et al., 1979).

Finally, on the basis of the findings with the model of 10-Å radius, the model parameters of the hemoglobin α chain and sperm whale myoglobin (requiring a sphere of 18 Å for both cases) were likewise adjusted as described below to test the contributions of charge distribution and static accessibility, SA, to the distinctive electrostatic properties of these two proteins.

Results and Discussion

Electrostatic Contributions to the Bohr Effect. The Bohr effect refers to excess binding of protons by deoxyhemoglobin relative to oxyhemoglobin at physiological pH and is therefore

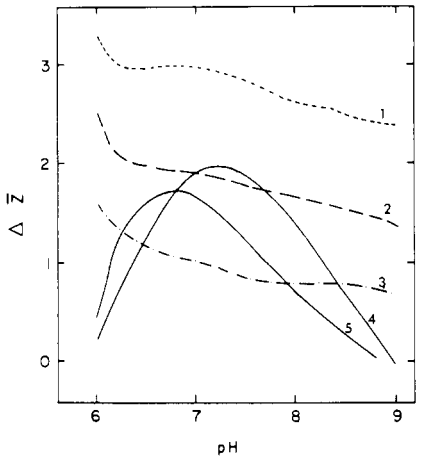

FIGURE 1: Electrostatically calculated contributions to the Bohr effect, $\Delta\bar{Z}$ vs. pH 6–9 at 25 °C, in human hemoglobin A excluding anion binding. Broken curves: (1) I = 0 M; (2) at I = 0.01 M; and (3) at I = 0.10 M. Full curves were drawn through the experimental data of Rollema et al. (1975), curve 4 in 0.10 M KCl and curve 5 in 0.01 M KCl.

expressed by the difference between the two separate titration curves [see, for example, Figures 4 and 5 of the preceding paper in this issue, Matthew et al. (1979)]. The computed difference curves, $\Delta\bar{Z}$, between deoxyhemoglobin and oxyhemoglobin against pH in the range 6–9 at 25 °C are shown in Figure 1. Curves 1, 2, and 3 represent the computed $\Delta\bar{Z}$ values for ionic strengths of 0.00, 0.01, and 0.10 M, respectively. No other factors, such as anion binding or subtle tertiary conformational effects, were taken into account at this stage. Curves 4 and 5 represent the experimentally observed Bohr effect (Rollema et al., 1975) for 0.10 and 0.01 M ionic strength, respectively. The strong ionic strength dependence of the computed results is clear from Figure 1. The computed curve differs from the corresponding experimental curve, e.g., curves 3 and 4 at 0.10 M ionic strength, both with respect to the magnitude of $\Delta\bar{Z}$ and its pH dependence. As shown below, the discrepancy is largely explained in terms of specific binding of anions.

Preferential Chloride Binding by Deoxyhemoglobin. As discussed above and elsewhere (de Bruin et al., 1974; Rollema et al., 1975; Arnone et al., 1976; O'Donnell et al., 1978; Matthew, 1978; Matthew et al., 1979), there is both direct and indirect evidence for the preferential binding of chloride ion by deoxyhemoglobin. Direct crystallographic evidence places a chloride ion at each of the two interchain sites Val-1α_1···Cl^-···Arg-141α_2 in the deoxyhemoglobin tetramer at the 0.10 M chloride level (Arnone et al., 1976). There is also indirect evidence for the additional binding of chloride ion at another site such as the His-117β region in each dimer (Tucker & Perutz, 1977). A corresponding binding of chloride ion to the oxyhemoglobin tetramer is confined to higher ionic strength (Rollema et al., 1975) or low pH outside of the range of the alkaline Bohr effect.

Figure 2 allows comparison of the experimentally determined Bohr effect in 0.10 M KCl, curve 3 (Rollema et al., 1975), with the computed effect shown in terms of two stages of inclusion of chloride binding to the deoxyhemoglobin. Curve 1 incorporates only the Val-1α_1···Cl^-···Arg-141α_2 site and accounts for approximately 75% of the total effect at its maximum relative to the observed curve 3. Curve 2 incorporates both chloride binding sites mentioned above. It predicts a bell-shaped curve with a maximum of 2.0 Bohr protons. A shift of curve 2 by 0.4 pH unit to improve the agreement with observation could be achieved by altering pK_{int}

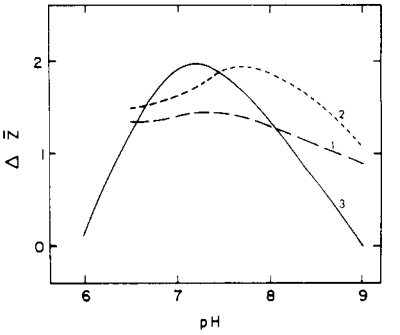

FIGURE 2: Electrostatically calculated contribution to the Bohr effect, as in Figure 1 but at constant ionic strength, I = 0.10 M, with inclusion of anion binding to deoxyhemoglobin. Curve 1 incorporates two bound Cl^- per tetramer at the Val-1α_1···Cl^-···Arg-141α_2 sites. Curve 2 incorporates four bound Cl^- per tetramer, two at the site above and two at His-117β···Cl^-Arg···30β. Curve 3 shows the corresponding experimental result at 0.10 M KCl, as in Figure 1.

values but at the expense of abandoning the generality of the treatment. Computations also show that the second binding site need not be restricted to His-117β; other plausible sites yield similar results. Similar treatment can be applied at lower and higher salt concentrations; however, as seen above no Cl^- binding need be invoked to account for observations at ionic strengths of 0.01 and below.

Acid Bohr Effect. At pH values below 6, excess binding of protons by oxyhemoglobin relative to deoxyhemoglobin is observed. At one time this effect was attributed to an abnormal decrease in acid strength of certain carboxyl groups of relatively high pK upon oxygenation of hemoglobin (Antonini et al., 1965). More recent work, however, has shown that the effect is linked to chloride ion binding, since it is diminished at low salt concentrations and almost vanishes in 0.005 M KCl (Rollema et al., 1975).

The present treatment (Matthew, 1978; Matthew et al., 1979) does not predict abnormally high pK values for any carboxyl groups in hemoglobin nor large differences in their pK on passing between deoxyhemoglobin and oxyhemoglobin. The predicted difference without allowing for chloride ion binding or tetramer dissociation (Atha & Riggs, 1976) is indeed in the opposite direction [Figure 1; see also Matthew et al. (1979)]. Because of the supervention of tetramer dissociation, no attempt will be made here to deal in detail with the acid Bohr effect.

Individual Site Contributions to Alkaline Bohr Effect. Details of the contributions of individual sites to the alkaline Bohr effect at pH 7.60 and 25 °C are shown in Table I. The residues listed are those primarily involved, comprising eleven histidine residues, two valine residues, and one lysine residue. The pK_i values at pH 7.60 for each residue in the deoxyhemoglobin and oxyhemoglobin forms are given, along with the difference, ΔZ, in proton equivalents bound to each group which represents its individual computed contribution per tetramer to the Bohr effect.

Table I shows that all the titrating groups participate in the Bohr effect, though to varying degrees. This is a thermodynamic consequence of the fact that the deoxy- and oxyhemoglobin structures have different charge geometries, so that each individual group is subject to different electrostatic forces that cause a different dependence on variations in pH and ionic strength. The relative magnitudes of their roles as Bohr groups are therefore variable. Although all listed residues contribute at zero ionic strength, at the 0.10 M level only five residues dominate, reflecting their special positions and/or interactions with ions.

Table I: Contributions to the Bohr Effect Determined by Electrostatic Calculation[a]

	I = 0.10 M			I = 0.01 M			I = 0 M
group	deoxy pK_i	oxy pK_i	Δz_i	deoxy pK_i	oxy pK_i	Δz_i	Δz_i
			α Chain				
Val-1	7.57	7.33	0.26	8.02	7.66	0.38	0.37
	(8.01)	7.33	(0.74)				
His-20	6.85	6.84	0.00	7.02	6.99	0.02	0.10
His-45	6.87	6.87	0.00	7.19	7.07	0.10	0.27
His-50	7.48	7.45	0.04	7.80	7.69	0.12	0.20
His-72	6.36	6.35	0.00	6.63	6.59	0.01	0.08
His-89	7.18	7.22	−0.03	7.51	7.47	0.04	0.16
His-112	7.70	7.67	0.03	8.05	7.95	0.09	0.13
			β Chain				
Val-1	7.03	6.78	0.16	7.22	6.76	0.34	0.59
His-2	6.68	6.68	0.00	6.82	6.70	0.06	0.14
His-77	6.64	6.59	0.02	6.74	6.58	0.07	0.15
His-117	7.74	7.71	0.03	8.03	7.93	0.09	0.14
	(8.19)	7.71	(0.46)				
His-143	6.27	4.55	0.09	6.42	4.40	0.12	0.20
His-146[b]	8.43	8.18	0.31	8.86	8.38	0.18	0.14
Lys-82	10.33	9.06	0.06	10.51	9.07	0.06	0.04
total			0.97			1.68	2.73
			(1.88)				

[a] I = 0, 0.01, and 0.10 M at T = 25 °C and pH 7.60. ΔZ_i = Bohr protons per tetramer. pK_i values are listed at 0.01 and 0.10 M ionic strengths. The effect of including Cl^- bound in deoxyhemoglobin at Val-1α and His-117β at I = 0.10 M is indicated within parentheses below the values calculated excluding ion binding. Totals are given on the bottom line. Data are rounded off to the second decimal. [b] His-146β imidazole···Asp-94β salt bridge is intact, the effect being due to proximity of interface transition.

As shown in Table I, a substantial contribution to the Bohr effect is attributed to Val-1α at pH 7.60. The effect is significant, 0.26 proton equiv, when chloride binding is neglected but is accentuated to 0.74 proton equiv if the nearby chloride ion site is taken to be occupied, as shown in parentheses in the table. A similar accentuation is computed for His-117β, although the evidence for this particular location for a second chloride equivalent bound is not conclusive. The contribution of His-146β is a general effect and does not depend on a special circumstance; recent work on hemoglobin Kansas (Kilmartin et al., 1978) shows that the quaternary transition in hemoglobin can occur without rupture of the His-146β···Asp-94β tertiary salt bridge. Since intrachain rearrangements are neglected at the present level of refinement, the molecular basis of the predicted proton binding behavior of His-146β is attributable to the rigid rotation of the β chain with respect to the α chain in the quaternary transition with the concomitant changes in charge disposition and solvent accessibilities.

Table I indicates a contribution of 0.16 proton equiv from Val-1β. The effect is slightly larger than expected from ^{13}C NMR measurements that do not indicate a significant pK_i difference between the deoxy- and oxyhemoglobin forms (Matthew et al., 1977; Matthew et al., 1979). Since there is experimental evidence discussed above for weak chloride binding at this site (Chiancone et al., 1976; Wiechelman et al., 1978), the effect of introducing a partially saturated anion site was tested for the oxyhemoglobin case at I = 0.10 M. This change in the computation basis readily reduced the Val-1β Bohr effect contribution to a negligible level. It is interesting that Lys-82β was computed to contribute 0.06 Bohr protons at pH 7.60 even though this pH is well beyond the usual titration range for lysine residues. Corresponding changes in other lysine pK_i values are not large enough to be considered at pH 7.60.

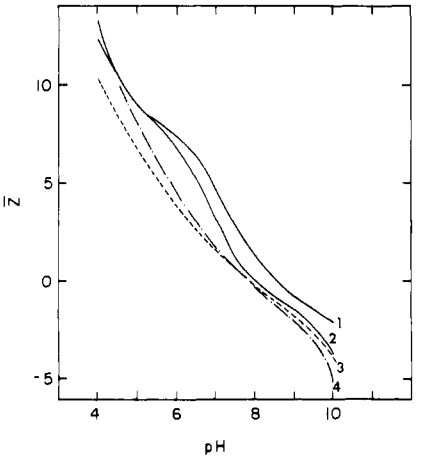

FIGURE 3: Comparison of ionic strength effects on titration curves, net protein charge $\bar{Z}$ vs. pH at 25 °C, for human ferrohemoglobin α-chain monomer (full curves, 1 and 2) and sperm whale ferromyoglobin (broken curves, 3 and 4). Curves 1 and 3 apply at I = 0 M and curves 2 and 4 at I = 0.10 M.

The computed electrostatic contributions at I = 0.10 M and pH 7.60 are seen to total 0.97 Bohr protons without Cl^- binding, representing 50% of the observed maximum Bohr effect, and 1.88 Bohr protons including bound Cl^- at two deoxyhemoglobin sites per dimer, nearly equal to the experimental value. At the 0.01 M salt level, there is no need to invoke Cl^- binding, since the computed 1.68 Bohr protons are not far from the experimental value (see Figure 1).

Nonclassical Ionic Strength Behavior of Hemoglobin Titration Curves. It was noted in the preceding paper in this issue [Matthew et al. (1979), Figure 4] that deoxyhemoglobin exhibited nonclassical electrostatic behavior, in that the part of its titration curve which showed a minimum ionic strength effect was far from the isoionic pH of 7.4, occurring instead near pH 5 (Steinhardt & Zaiser, 1955; Tanford, 1965). To answer the question whether the abnormal behavior is a feature of the hemoglobin quaternary structure or an inherent property of its monomer polypeptide chains or a combination of both, we compared the calculated ionic strength variation of hydrogen ion titration curves of human deoxyhemoglobin α chain (Matthew et al., 1978a; Matthew, 1978) and sperm whale ferromyoglobin (Nakhleh, 1971; Shire et al., 1974a,b). The titration curves were calculated at three ionic strength levels: 0.0, 0.01, and 0.10 M. The results at I = 0.0 and 0.10 M are shown in Figure 3 (the intermediate curves at 0.01 M fitted the pattern but were omitted for clarity). The myoglobin curves, 3 and 4, are seen to cross near the isoionic pH 8, as expected, whereas hemoglobin α chain, curves 1 and 2, exhibits the nonclassical behavior, the curves crossing near pH 5. This behavior of the hemoglobin α chain is sufficiently like that of the deoxyhemoglobin tetramer that the simpler monomeric form is used to explore the basis of the nonclassical behavior. It was assumed that no chloride ion binding sites were occupied in these monomeric forms under the conditions of the comparisons.

The question now follows as to whether these observations reflect the properties of the individual titrating groups. We therefore compared the predicted ionic strength variation of the individual titration curves for a number of amino acid residues in hemoglobin α chain with their equivalent groups in myoglobin. The same phenomenon was observed, namely, classical behavior by individual groups in myoglobin but not in hemoglobin α chain. Figure 4 shows the computed behavior for the Val-1 group in both proteins. As expected, the variation of ionic strength dependence of pK_i with pH is strongest at

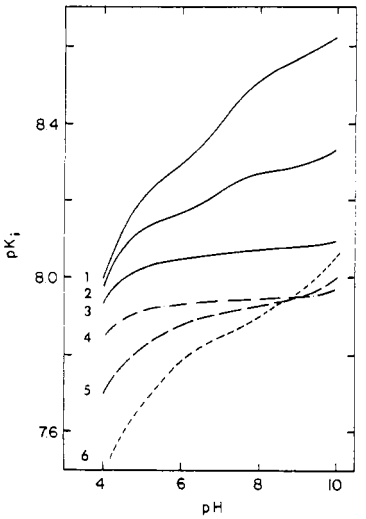

FIGURE 4: Comparison of ionic strength effect on the electrostatically calculated pK_i values for a single amino acid residue, the amino-terminal valine group, in human ferrohemoglobin A α-chain monomer (solid curves, 1, 2, and 3) and sperm whale ferromyoglobin (broken curves, 4, 5, and 6). The pH variation at 25 °C is shown at three levels of ionic strength: 0 M, curves 1 and 6; 0.01 M, curves 2 and 5; and 0.1 M, curves 3 and 4.

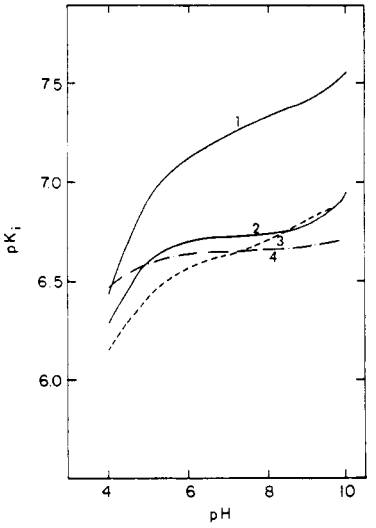

FIGURE 5: Comparison of ionic strength effect on the electrostatically calculated pK_i values for His-112α in the hemoglobin α chain (curves 1 and 2) and for His-48 in ferromyoglobin (curves 3 and 4). Conditions are as in Figure 4, but only two ionic strength levels are shown: I = 0.0, curves 1 and 3, and 0.10 M, curves 2 and 4.

the lowest ionic strength, I = 0 M, and is weakest at the highest, I = 0.1 M, in both cases. However, the three Val-1 curves intersect near pH 8.4 in myoglobin (curves 4, 5, and 6), whereas the corresponding curves in hemoglobin α chain (curves 1, 2, and 3) meet near pH 4. Figure 5 presents the equivalent comparison for representative histidine residues, 112α in hemoglobin and 48 in myoglobin, plotted at two ionic strengths for clarity and showing the same contrast as for the NH_2 termini. Other groups follow the pattern. It appears that the fundamental difference in ionic strength behavior between hemoglobin and myoglobin may lie not so much in the oligomeric protein structure or in the chemical nature of the charged groups themselves as in their unique distributions (Nagasawa & Holzer, 1964).

Comparison of Spatial Distribution and Solvent Accessibility of Charged Groups in Hemoglobin and Myoglobin. To explore the basis for the nonclassical behavior of hemoglobin the following detailed comparison of hemoglobin α chain and sperm whale ferromyoglobin is helpful. In terms of composition, hemoglobin α chain and myoglobin contain respectively 15 and 24 acid groups, 14 and 23 strongly basic groups, and 9 and 8 more neutral groups comprising histidine and NH_2-terminal valine residues. Including tyrosine residues, hemoglobin α chain musters 41 titratable groups to 59 for myoglobin. This translates for an 18-Å radius sphere to a surface area per chargeable group of 100 Å for hemoglobin α chain and 70 Å for myoglobin. For a uniform charge distribution, r_{ij} between nearest neighbors averages to 10 and 8.3 Å, respectively.

Table II: Charge-Pair Relationships in Sperm Whale Ferromyoglobin and Hemoglobin α Chain[a]

sperm whale myoglobin			hemoglobin α chain		
AA	r_{ij}	base	AA	r_{ij}	base
Glu-4	2.4	Lys-79	Asp-6	3.1	Lys-127
Glu-6	2.8	Lys-133		6.8	Val-1
Glu-18	3.5	Lys-77	Glu-23	5.7	His-112
Asp-20	4.1	Arg-118		6.5	His-20
Asp-27	3.3	Arg-118	Glu-27	3.20	Arg-31
Glu-38	2.8	His-36		3.3	His-112
Glu-41	5.4	Lys-47	Glu-30	2.4	His-50
	5.5	Lys-50	Asp-47		
Asp-44	3.3	Lys-47	Asp-64	6.8	Lys-60
Glu-52	4.6	Lys-56	Asp-74	2.8	Lys-7
	5.2	Lys-34		6.2	Lys-11
Glu-54			Asp-75	6.0	His-72
Glu-59	5.5	Lys-62	Asp-85	2.9	Lys-139
Asp-60	3.1	Arg-45		4.2	His-89
Glu-83	6.5	His-81	Asp-94		
	6.6	Lys-78	Glu-116	3.9	Lys-16
Glu-85			Asp-126	6.2	His-112
Glu-105	3.8	Lys-102			
Glu-109			C term		
Asp-122	3.4	Lys-16	heme PR1	4.5	Lys-61
Asp-126	6.2	His-122	heme PR2	3.7	His-45
Glu-136	5.5	Arg-139			
Asp-141	3.3	Lys-140			
	5.1	Lys-141			
Glu-148					
C term					
heme PR1	6.1	Lys-96			
heme PR2	6.2	Arg-45			

[a] r_{ij} denotes the separation in angstroms between point charges.

In both proteins the r_{ij} between nearest neighbors bearing opposite charges is less than the distance prescribed by uniform charge distribution. Table II lists all the acidic functions in the hemoglobin α chain and myoglobin with their positively charged neighbors wherever $r_{ij} < 7.0$ Å. Table II shows clearly that histidine residues in hemoglobin α chain are generally much closer to acid groups than they are in myoglobin. These differences are reflected in the higher $pK_{1/2}$ values seen for histidine residues in hemoglobin tetramer (Ho & Russu, 1978) than in myoglobin (Botelho et al., 1978), as summarized in the preceding paper in this issue (Matthew et al., 1979).

The distinction between hemoglobin α chain and myoglobin applies also to the mean static solvent accessibilities, $\overline{SA}$, of the different classes of charge-bearing groups. The $\overline{SA}$ values respectively for hemoglobin α chain and myoglobin are 0.46 and 0.54 for acidic residues, 0.73 and 0.52 for strongly basic residues, and 0.53 and 0.68 for the more neutral basic groups. The lower $\overline{SA}$ values for acidic and neutral residues in the hemoglobin α chain reflect in part their mutual interaction according to the pairing in Table II and further contribute to raising the $pK_{1/2}$ values for the histidine residues. At the same time the strongly basic residues in hemoglobin α chain are relatively less closely paired with acidic residues and also have

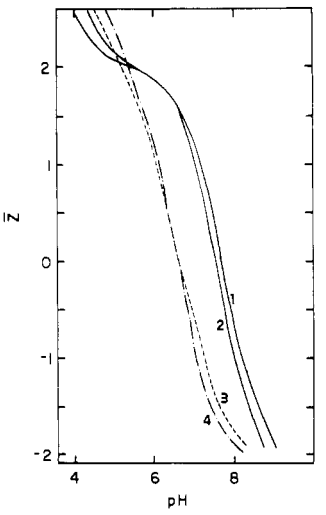

FIGURE 6: Simulated titration curves for a hypothetical polyelectrolyte model having 14 point charges placed on a sphere of radius 10.0 Å. The charges were assigned to three types: six carboxylic acids, pK_{int} = 4.00; four imidazoles, pK_{int} = 6.60; and four amines, pK_{int} = 10.00. Curves 1 and 2 correspond to a paired-charge distribution, at 0 and 0.10 M ionic strength, respectively. Curves 3 and 4 correspond to a uniform charge distribution, at 0 and 0.10 M ionic strength, respectively. See text for explanation.

a distinctly larger $\overline{SA}$ than in myoglobin. These observations are functionally significant, since on the one hand the higher $pK_{1/2}$ values of histidine residues contribute to buffering in the appropriate pH range (Matthew et al., 1979) and on the other hand the greater $\overline{SA}$ of strongly basic groups provides the mechanical exposure that facilitates the stabilization of hemoglobin subunit contacts through such side chains as Arg-31α, Lys-40α, Arg-92α, Lys-127α, and Arg-141α with β-chain components.

Simulated Model of Titration Behavior of Hemoglobin α Chain and Ferromyoglobin. Figure 6 compares the simulated titration curves for two hypothetical polyelectrolyte models chosen to mimic the charge distributions and $\overline{SA}$ values characteristic of hemoglobin α chain and myoglobin. The paired charge model is shown by curves 1 and 2 for ionic strengths of 0.00 and 0.10 M, respectively, and the uniform distribution model is shown by curves 3 and 4 for the corresponding ionic strength values. The model consists of 14 point charges placed on a sphere of radius 10.0 Å. The charges are assigned to three types: six carboxylic acids of pK_{int} = 4.00; four imidazoles, pK_{int} = 6.60; and four amines, pK_{int} = 10.00. The paired-charge, nonclassical pattern of curves 1 and 2 was achieved by placing the carboxylic and amine charges at the vertexes of the inscribed regular polygon (see Electrostatic Computations) but with the imidazoles located with maximum symmetry on the spherical surface 3.0 Å from carboxylate points. The classical pattern of curves 3 and 4 placed all 14 charges at the vertexes of the inscribed polygon which increased the distance between each imidazole point charge and the nearest carboxylate point charge to approximately 6.5 Å. The nonpaired charges were assigned SA values of 0.50, while the SA values of members of charge pairs were taken as 0.20.

The broken curves 3 and 4 in Figure 6 for the uniform geometry of point charges show, classically, a minimum sensitivity to ionic strength near $\bar{Z}$ = 0, whereas the nonuniform geometry represented in the solid curves 1 and 2 produces a nonclassical minimum sensitivity to ionic strength well displaced from the region of $\bar{Z}$ = 0. The characteristics of these curves, therefore, mimic the effects seen for the hemoglobin α chain and myoglobin in Figure 3 for correspondingly designated curves.

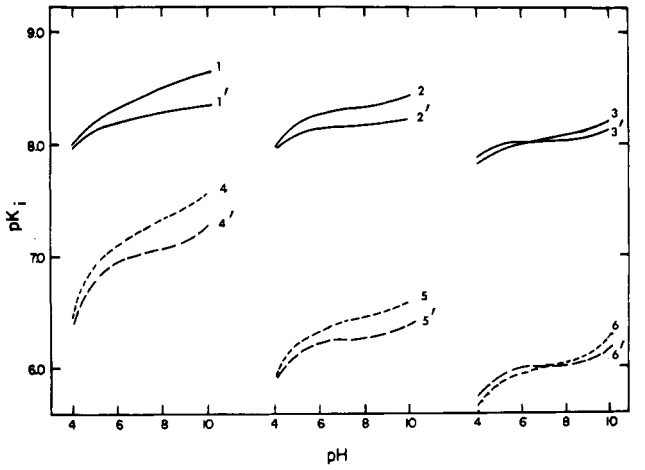

FIGURE 7: Shown are the pH and ionic strength dependences of two groups in the hemoglobin α chain: Val-1α (curves 1–3) and His-112α (curves 4–6). Unprimed and primed numbers indicate the 0 and 0.01 ionic strength calculations, respectively. The two sets of curves designated 1 and 4 show the predicted pK_i behavior in hemoglobin α chain for Val-1α and His-112α, respectively. Curves 2 and 5 show the predicted behaviors when the α-chain charge configuration is altered by splitting the histidine–carboxyl ion pairs to 10-Å distance. Finally, curves 3 and 6 show the predicted behaviors for Val-1α and His-112α when, in addition, the static accessibility of each lysine and arginine point charge is reduced from an average of 0.73 to 0.50. The two steps in altering the characteristic charge pattern of hemoglobin α chain render it in stages similar to that of myoglobin.

Hypothetical Manipulation of Hemoglobin α Chain Electrostatic Characteristics. Comparison of the protein titrations in Figure 3 with the simulations in Figure 6 suggests that hypothetical manipulation of the hemoglobin α chain charge and SA configurations could yield the classical myoglobin-like titration behavior. It is convenient to show the manipulation in two steps. In the first step the near-neighbor carboxyl groups (Table II) are arbitrarily moved away from all imidazole groups to a distance of 10 Å. In practice this change enhances the interaction between the carboxyl and the basic arginine and lysine groups. In the second step the $\overline{SA}$ for the latter basic residues was reduced from 0.73 to 0.50 to mimic the further effect of reduced SA on the interaction between those strongly basic residues and the carboxyl groups as seen in myoglobin.

The effects of these two steps of hypothetical manipulation are shown for the previously discussed two representative groups in the hemoglobin α chain, Val-1α and His-112α. Figure 7 shows the ordinate as the computed pK_i for Val-1α, above, and for His-112α, below, with the pH abscissa divided into three sections. The left-hand section (curves 1 and 4) applies to the observed, unperturbed geometry; the middle section (curves 2 and 5) applies to the charge system constructed by moving the carboxyl groups to increase r_{ij} for the separation of the paired imidazole and carboxyl groups (Table II) to 10.0 Å; the right-hand section (curves 3 and 6) applies to the structure obtained when, in addition, the lysine and arginine point charges are all given the SA value of 0.50. For each case the upper numbered curve applies to ionic strength 0.00 M and the lower primed curve applies to ionic strength 0.01 M. Curves 1 and 1′ correspond to curves 1 and 2 in Figure 4, and curves 4 and 4′ correspond (except for an ionic strength difference) to curves 1 and 2 in Figure 5. In all cases increased ionic strength flattens the computed curves.

The upper (solid) curve sets in Figure 7 for the Val-1α site show definite decreases in pK_i (curves 2 and 2′) as the carboxyl group positions are altered in a way that reduces their summed

interactions with the site in question [compare with Figure 2 of Matthew et al. (1979)]. The second step (curves 3 and 3′) shows that reducing the SA of the positively charged lysine and arginine residues further lowers pK_i values for the Val-1α site and shifts the ionic strength dependence much more toward the classical minimum near $\bar{Z} = 0$. Both these effects are even more pronounced in the case of His-112α. As Table II shows, His-112α is a strong candidate for this effect in that Glu-23α and Glu-27α are in its near vicinity; however, the situation is not unique to this histidine residue. Qualitative comparison with Figure 3 of the preceding paper in this issue may be useful (Matthew et al., 1979). Note that in Figure 7 curves 3 and 3′ bear similarities with curves 6 and 5 in Figure 4, and curves 6 and 6′ are similar to curves 3 and 4 in Figure 5, in each case again attesting to successful manipulation of the hemoglobin α chain charge configuration to mimic the titration behavior of individual groups in myoglobin. The overall titration curves predicted for these charge manipulations follow the behavior of the individual sites.

Despite the overall secondary and tertiary structural similarities between myoglobin and the hemoglobin subunits, it is clear that the differences in charge distributions and the associated solvent accessibilities confer unique functional properties. As indicated in Figure 7, the pairing of oppositely charged groups characteristic of the hemoglobin α chains exaggerates the ionic strength dependence of pK_i of various groups and of the aggregate titration curve in the region of $\bar{Z} = 0$. Similar simulations, to be published separately, show that with a charge configuration characteristic of cytochrome *c*, an ionic strength dependence observable near $\bar{Z} = 0$ will be introduced by the pairing of the carboxyl groups with lysine side chains. In either case the sensitivity of the ion-pair interaction to the presence of mobile ions in the solvent is responsible in part for the nonclassical sensitivity to variation in ionic strength.

As indicated further in Figure 7, the systematic differences in $\overline{SA}$ between classes of groups will contribute strongly to the nonclassical behavior. This is easily understood in qualitative terms. The charged groups with larger values of SA_j [eq 3 of Matthew et al. (1979)] contribute proportionally smaller W'_{ij} terms, so that their summed contribution is relatively weak in comparison with their numbers. The hemoglobin α chain, therefore, must acquire a net positive formal charge to reach an effective balance, because $\overline{SA}$ for lysine and arginine residues, at 0.73, is much larger than that for glutamic and aspartic acid residues, 0.46. The latter are only partially offset by the less numerous histidine residues, $\overline{SA} = 0.53$. As Figure 7 shows, altering the $\overline{SA}$ for lysine and arginine residues to the comparable value of 0.50 has a decisive effect in minimizing the ionic strength dependence at $\bar{Z} = 0$. These observations underscore very vividly the importance of the static solvent accessibility analysis that was introduced by Lee & Richards (1971) and first applied to electrostatic interactions by Shire et al. (1974a,b, 1975).

The overall low surface charge density of the hemoglobin α chains further helps accentuate the electrostatic interactions by providing a relatively ineffective shielding array (S. H. Friend and F. R. N. Gurd, unpublished experiments) after allowance is made for the larger average r_{ij} values. Note also that the proximity of charge sites within about 6.4 Å of each other, characteristic of charge pairing, generally will lessen their solvent accessibility and thus the effective dielectric through which their Coulombic properties make themselves felt.

Interpretation of the Bohr Effect. The preceding discussion has shown in principle how the unequal hydrogen ion binding by deoxyhemoglobin and oxyhemoglobin in the physiological pH range can be attributed at physiological ionic strength to the interaction between all charged groups on the molecule in the two quaternary structural states. Specific chloride ion binding is clearly implicated. The charge distributions on the two hemoglobin quaternary structures are each unique and differ from each other both in terms of separations between charged sites, r_{ij}, and differences in static solvent accessibility, SA. These structural differences lead to significant differences in the free energy of interaction between pairs of charged groups, W'_{ij}, and so require that hydrogen ion binding under given conditions will differ also.

The transformation of electrostatic configuration from deoxyhemoglobin to produce a lower proton affinity and lesser sensitivity to ionic strength illustrates the operation of the same factors as in the comparison made above at the monomeric level between the ferroheme forms of hemoglobin α chain and myoglobin. As shown in Tables III–V of the preceding article in this issue (Matthew et al., 1979), the factors that are altered during the transformation from deoxyhemoglobin to oxyhemoglobin are not simply the changes in r_{ij} values upon subunit rotation and translation but also the changes in SA values for three, seven, and three sites in the sets corresponding to acid groups, strongly basic groups, and relatively neutral groups, respectively, per $\alpha\beta$ dimer. Particularly notable is the fact that the difference in $\overline{SA}$ between the negatively and positively charged sets of groups, which is 0.14 in deoxyhemoglobin, is reduced by 30% to 0.10 in oxyhemoglobin. These changes produce a more balanced electrostatic interaction pattern in the oxyhemoglobin than in the deoxyhemoglobin charge configuration. The changes occur without alteration of r_{ij} between any histidine imidazole residue and its nearest negatively charged neighbor with which it can be considered to form an ion pair. The resultant of these quaternary structural changes involving r_{ij} values and particularly SA values is felt most strongly by relatively few groups, the five most sensitive groups discussed above in connection with Table I.

The less symmetric deoxyhemoglobin charge configuration is more sensitive to ionic strength [Figures 4 and 5 of the preceding paper, Matthew et al. (1979)]. The alkaline Bohr effect, defined by the difference curve, decreases with ionic strength (Figure 1). This trend is complicated by the preferential binding of chloride to the deoxyhemoglobin tetramer, one or more anion binding sites being saturated at 0.10 M chloride. This differential anion binding enhances the alkaline Bohr effect. Its contribution overtakes the diminishing ionic strength component by $I = 0.10$ M. These factors account approximately for the observed ionic strength variation of the Bohr effect up to 0.10 M KCl, while at higher chloride concentrations anion binding to oxyhemoglobin becomes substantial (Rollema et al., 1975).

These chloride ion interactions studies, when taken with recent proton NMR studies (Ho & Russu, 1978) and discrete charge p*K* calculations, yield a new view of the stereochemical model for the alkaline Bohr effect (Perutz, 1970) and the individual contributions of His-146β and Val-1α (Kilmartin et al., 1973a; Kilmartin & Rossi-Bernardi, 1973; Kilmartin, 1977; Perutz et al., 1969; Perutz, 1978b). Previous interpretations have attributed 70–80% of the observed alkaline Bohr effect at pH 7.4, ionic strength of 0.10 M, to Val-1α and His-146β, approximately 30 and 40%, respectively. These estimates were based on experimentally determined p*K* values

under nonequivalent conditions (Garner et al., 1975; Kilmartin et al., 1973a,b; Matthew et al., 1977). It is now known that a chloride concentration of 0.10 saturates the Val-1α chloride binding site, thereby maximizing the Val-1α Bohr effect contribution. The evidence supporting the rupture of the His-146β···Asp-94β salt bridge only at ionic strengths greater than 0.10 was discussed above. It has been shown (Table I and Figure 2) that the entire alkaline Bohr effect can be accounted for without invoking tertiary rearrangements. At chloride ion concentrations greater than 0.10, where specific chloride binding to oxyhemoglobin reduces the observed alkaline Bohr effect (Rollema et al., 1975), the rupture of the His-146β salt bridge may preserve the deoxy-to-oxyhemoglobin hydrogen ion binding differential. The development of highly refined crystallographic data (Perutz, 1963; Perutz et al., 1968; Muirhead & Greer, 1970; Bolton & Perutz, 1970; Fermi, 1975) has been of paramount importance for the design and interpretation of hemoglobin solution studies.

Conclusion

The adaptation of the discrete-charge electrostatic model (Tanford & Kirkwood, 1957) to include the static solvent accessibility parameter (Lee & Richards, 1971) correlated well with the then unassigned p$K_{1/2}$ values in several myoglobins (Shire et al., 1974a,b). The model dealt effectively with the ionic strength dependence of the hemic acid dissociation of several ferrimyoglobins (Shire et al., 1975). The treatment was refined to deal specifically with particular charge-bearing atoms rather than with side chains as a whole, and the choice of histidine imidazole nitrogen atoms as charge-bearing sites was systematized (Botelho, 1975). A faster, more economical algorithm was developed for estimation of SA (Matthew et al., 1978a). After the assignment of p$K_{1/2}$ values for histidines in 12 distinguishable myoglobin species (Botelho & Gurd, 1978), the predictive value of the model could be established in detail (Botelho et al., 1978). The conclusion that structural similarities among the myoglobins persist over a range of species is supported by the recent crystallographic results of Scouloudi (Scouloudi & Baker, 1978; Scouloudi, 1978). The electrostatic treatment was shown to be applicable to cytochrome *c* and the hemoglobin α chain with the identical set of pK_{int} values as were used for the myoglobins (Matthew et al., 1978b).

In this paper and the preceding one in this issue (Matthew et al., 1979), the treatment is extended to the human deoxyhemoglobin and oxyhemoglobin tetramers. The computed results fit with observations over the whole titration range in which the native structures remain intact. The match of computed and observed pK values (Ho & Russu, 1978) is good for the terminal valine residues in each tetrameric structure as well as for histidine residues where their experimental pK values have been assigned. Not only do the assigned values for histidine residues bracket the high and low pK limits for the observed and calculated values but also the special sensitivity of His-143β to quaternary state is predicted by the theory. The treatment deals nearly quantitatively with the alkaline Bohr effect in terms of differences in the charge configuration between the deoxyhemoglobin and oxyhemoglobin tetrameric structures. Estimates of the contributions of two or four bound chloride ions differentially bound by the deoxyhemoglobin tetramer are included in the computations. The differences in charge configuration between the tetrameric hemoglobin structures involve important changes in SA of 26 charge-bearing sites. These differences explain the ionic strength dependence of the Bohr effect and the strikingly nonclassical relationship in hemoglobin between ionic strength dependence and net protein charge. The latter effects were simulated in terms of the comparison between the monomeric hemoglobin α chain and the sperm whale myoglobin as well as with appropriate formal models.

The value of the present results lies not only in the explanations that they offer for many phenomena observed with hemoglobin but also in demonstrating the applicability of a general treatment for approximately spherical proteins of known three-dimensional structure. The treatment provides a context for interpretation of electrostatic effects. Singular observations taken out of context may lead to oversimplified interpretations. Knowles (1976) has described examples in which the pH dependence of enzyme activity has been correlated incorrectly with binding of protons by individual sites. The behavior of individual sites has often been interpreted in terms of relationships only with near neighbors, with the underlying assumption that r_{ij} was dominant and that SA_j could be neglected (Perutz, 1978a,b). While this type of effect may dominate at high ionic strength (I = 1.0 M), the possibility of interactions among constellations of charged groups in the protein remains. At ionic strength values where our computations apply (Tanford, 1957; Olivares & McQuarrie, 1977), the influence of numerous single sites prevails (Matthew et al., 1979). Lack of ionic strength effects in this range may be taken as an indication of lack of electrostatic interaction (Tanford & Roxby, 1972). However, as the present work illustrates, such a result may arise from the interplay of offsetting specific and general ion effects.

The heterotropic effectors of hemoglobin, like the majority of known allosteric effectors, produce changes in the state and distribution of the protein charges. The electrostatic interactions involving hydrogen ions dealt with here will be extended to the carbamino and organic phosphate counterparts in a subsequent publication. The electrostatic contribution to the free energy of stabilization, obtained by summing, W'_{ij} terms, will be considered. Attention will also be given to the electrostatic consequences of residue substitutions in mutant hemoglobins. A case in point is sickle-cell hemoglobin. The SA of Glu-6β in hemoglobin A is high, approximately 0.95. Accordingly, its replacement by the uncharged Val-6β of hemoglobin S would be expected to produce a minimal electrostatic perturbation, as actually observed in terms of little or no alteration of pK values of histidine residues (Ho & Russu, 1978).

Acknowledgments

Helpful discussions with our co-workers Drs. R. A. Bogardt, R. J. Wittebort, T. M. Rothgeb, B. N. Jones, and Mr. S. H. Friend are gratefully acknowledged.

References

Antonini, E., Wyman, J., Brunori, M., Fronticelli, C., Bucci, E., & Rossi-Fanelli, R. (1965) *J. Biol. Chem. 240*, 2262.

Arnone, H., O'Donnell, S., & Schuster, T. (1976) *Fed. Proc., Fed. Am. Soc. Exp. Biol. 35*, 1604.

Atha, D. H., & Riggs, A. (1976) *J. Biol. Chem. 251*, 5537.

Bohr, C., Hasselbalch, K. A., & Krogh, A. (1904) *Skand. Arch. Physiol. 16*, 402.

Bolton, W., & Perutz, M. F. (1970) *Nature (London) 228*, 551.

Botelho, L. H. (1975) Ph.D. Thesis, Indiana University, Bloomington, IN.

Botelho, L. H., & Gurd, F. R. N. (1978) *Biochemistry 17*, 5188.

Botelho, L. H., Friend, S. H., Matthew, J. B., Lehman, L. D., Hanania, G. I. H., & Gurd, F. R. N. (1978) *Biochemistry 17*, 5197.

Chiancone, E., Norne, J. E., Forsen, S., Mansouri, A., & Winterhalter, K. H. (1976) *FEBS Lett. 63*, 309.
de Bruin, S. H., Rollema, H. S., Janssen, L. H. M., & van Os, G. A. J. (1974) *Biochem. Biophys. Res. Commun. 58*, 210.
Fermi, G. (1975) *J. Mol. Biol. 13*, 237.
Garner, M. H., Bogardt, R. A., Jr., & Gurd, F. R. N. (1975) *J. Biol. Chem. 250*, 4398.
Gros, G., & Bauer, C. (1978) *Biochem. Biophys. Res. Commun. 80*, 56.
Hayashi, A., Suzuki, T., & Stamatoyannopoulos, G. (1974) *Biochim. Biophys. Acta 351*, 453.
Ho, C., & Russu, I. M. (1978) in *Clinical and Biochemical Aspects of Hemoglobin Abnormalities* (Caughey, W. S., Ed.) p 179, Academic Press, New York.
Kilmartin, J. V. (1977) *Trends Biochem. Sci. 2*, 247.
Kilmartin, J. V., & Rossi-Bernardi, L. (1973) *Physiol. Rev. 53*, 836.
Kilmartin, J. V., Breen, J. J., Roberts, G. C. K., & Ho, C. (1973a) *Proc. Natl. Acad. Sci. U.S.A. 70*, 1246.
Kilmartin, J. V., Fogg, J., Luzzano, M., & Rossi-Bernardi, L. (1973b) *J. Biol. Chem. 248*, 7039.
Kilmartin, J. V., Anderson, N. L., & Ogawa, S. (1978) *J. Mol. Biol. 123*, 71.
Knowles, J. R. (1976) *CRC Crit. Rev. Biochem. 4*, 165.
Lee, B., & Richards, F. M. (1971) *J. Mol. Biol. 55*, 379.
Matthew, J. B. (1978) Ph.D. Thesis, Indiana University, Bloomington, IN.
Matthew, J. B., Morrow, J. S., Wittebort, R. J., & Gurd, F. R. N. (1977) *J. Biol. Chem. 252*, 2234.
Matthew, J. B., Hanania, G. I. H., & Gurd, F. R. N. (1978a) *Biochem. Biophys. Res. Commun. 81*, 410.
Matthew, J. B., Friend, S. H., Botelho, L. H., Lehman, L. D., Hanania, G. I. H., & Gurd, F. R. N. (1978b) *Biochem. Biophys. Res. Commun. 81*, 416.
Matthew, J. B., Hanania, G. I. H., & Gurd, F. R. N. (1979) *Biochemistry* (preceding paper in this issue).
Muirhead, H., & Greer, J. (1970) *Nature (London) 228*, 516.
Nagasawa, M., & Holtzer, A. (1964) *J. Am. Chem. Soc. 86*, 531.
Nakhleh, E. T. (1971) Ph.D. Thesis, American University of Beirut.
O'Donnell, S., Mandaro, R., & Schuster, T. (1978) *Biophys. J. 21*, 201a.
Olivares, W., & McQuarrie, D. A. (1977) *Chem. Phys. Lett. 46*, 178.
Perutz, M. F. (1963) *Science 140*, 863.
Perutz, M. F. (1970) *Nature (London) 228*, 726.
Perutz, M. F. (1978a) *Science 201*, 1187.
Perutz, M. F. (1978b) *Sci. Am. 239*, 92.
Perutz, M. F., Muirhead, H., Cox, M., & Goaman, C. G. (1968) *Nature (London) 219*, 131.
Perutz, M. F., Muirhead, H., Mazzarella, L., Crowther, R. A., Greer, J., & Kilmartin, J. V. (1969) *Nature (London) 222*, 1240.
Rollema, H. S., de Bruin, S. H., Janssen, L. H. M., & van Os, G. H. J. (1975) *J. Biol. Chem. 250*, 1333.
Scouloudi, H. (1978) *J. Mol. Biol. 126*, 661.
Scouloudi, H., & Baker, E. H. (1978) *J. Mol. Biol. 126*, 637.
Shire, S. J., Hanania, G. I. H., & Gurd, F. R. N. (1974a) *Biochemistry 13*, 2967.
Shire, S. J., Hanania, G. I. H., & Gurd, F. R. N. (1974b) *Biochemistry 13*, 2974.
Shire, S. J., Hanania, G. I. H., & Gurd, F. R. N. (1975) *Biochemistry 14*, 1352.
Steinhardt, J., & Zaiser, E. (1955) *Adv. Protein Chem. 10*, 151.
Tanford, C. (1957) *J. Am. Chem. Soc. 79*, 5340.
Tanford, C. (1965) in *Physical Chemistry of Macromolecules*, p 526, Wiley, New York.
Tanford, C., & Kirkwood, J. G. (1957) *J. Am. Chem. Soc. 79*, 5333.
Tanford, C., & Roxby, R. (1972) *Biochemistry 11*, 2192.
Tucker, P. W., & Perutz, M. F. (1977) *J. Mol. Biol. 114*, 415.
Wiechelman, K. J., Fox, J., McCurdy, P. R., & Ho, C. (1978) *Biochemistry 17*, 791.